

## A Benzodithiophene-based Semiconducting Polymer for Organic Thin Film Transistor

Jung-A Hong,<sup>†</sup> Ran Kim, Hui-Jun Yun,<sup>†</sup> Joung-Man Park,<sup>†</sup> Sung Chul Shin, and Yun-Hi Kim<sup>\*</sup>

*Department of Chemistry and RINS, Gyeongsang National University, Jinju 660-701, Korea. \*E-mail: ykim@gnu.ac.kr*

*<sup>†</sup>School of Material Science & Engineering and ERI, Gyeongsang National University, Jinju 660-701, Korea*

*Received December 28, 2012, Accepted January 24, 2013*

Benzodithiophene based organic semiconducting polymer was designed and synthesized by stille coupling reaction. The structure of polymer was confirmed by NMR and IR. The weight average molecular weight ( $M_w$ ) of polymer was 8,400 using GPC with polydispersity index of 1.4. The thermal, optical and electrochemical properties of polymer were characterized by TGA and DSC, UV-vis absorption and cyclic voltammetry. OTFT device using PBDT-10 exhibited the mobility of  $7.2 \times 10^{-5} \text{ cm}^2 \text{ V}^{-1} \text{ s}^{-1}$  and  $I_{\text{on}}/I_{\text{off}}$  of  $2.41 \times 10^3$ . The film morphology and crystallinity of PBDT-10, was studied using AFM and XRD.

**Key Words :** Organic semiconductor, Organic thin film transistors (OTFTs), Benzodithiophene

### Introduction

Organic thin film transistors (OTFTs) are all the more impressive because it is important factor for electronic applications such as active-matrix displays and flexible electronic devices, radio frequency identification (RFID) tags, smart cards, electronic papers, and sensors.<sup>1-6</sup> The OTFTs have been developed for large-area and low-cost electronics using liquid patterning and deposition techniques has fueled active research in printed electronics.<sup>7-10</sup> Organic semiconductors can be used as active layer by simple solution process, most of the reported devices were fabricated using a spin-coated polymer.<sup>11,12</sup> In this regard, to make  $\pi$ -conjugated polymeric materials soluble in common organic solvents, alkyl side chains are usually introduced onto their main chains.<sup>13-15</sup> A typical polymer semiconductor is poly(3-hexylthiophene) (P3HT), which was shown to provide a mobility of  $\sim 0.1 \text{ cm}^2 \text{ V}^{-1} \text{ s}^{-1}$ .<sup>16-18</sup> Many polythiophene derivatives have been studied because polythiophene can make planar backbone. However, the control of the region-regularity is very difficult.<sup>19-22</sup>

Recently, bithiophenes reporting a center aromatic ring was selected as a template, since the large planar benzodithiophene (BDT) unit has manufactured several high mobility semi-crystalline polymers, and the flanking thiophenes would lower steric hindrance and create smaller dihedral angles with adjacent monomers.<sup>23</sup> In addition, the symmetric nature of the BDT monomers eliminates the need to control the regioregularity during the polymerization process. The present conditions BDT derivatives as semiconductors in OTFT were reported with diverse alkyl substituents.<sup>24-27</sup>

In this paper, we designed and synthesized a poly(4,8-didecylthienobenzene-*alt*-dithiophene) (PBDT-10) as a polymer-semiconductor. The newly designed polymer is expected to have good morphology and charge carrier mobility due to the planar backbone between BDT and bithiophene without twist. The designed PBDT-10 was anticipated to have deep highest occupied molecular orbital (HOMO) level,

leading to higher stability than P3HT. Furthermore, conjugation length was extended through the bithiophene, which increases the intermolecular  $\pi$ - $\pi$  stacking characteristics.

### Experiment

**Measurements.** The  $^1\text{H}$ -NMR spectra was recorded on a Bruker Avance 300-MHz NMR spectrometer, respectively. UV-visible absorption was obtained using a Perkin Elmer LAMBDA-900 UV visible spectrometer. Cyclic voltammetric measurements were recorded using Epsilon E3 at room temperature in a 0.1 M solution of tetrabutyl-ammonium perchlorate ( $\text{Bu}_4\text{NClO}_4$ ) in acetonitrile under nitrogen gas protection at a scan rate of 50 mV/s. A Pt wire was used as a counter electrode and an  $\text{Ag}/\text{AgNO}_3$  electrode was used as the reference electrode. A thermogravimetric analysis (TGA) was performed under nitrogen using TA Instruments 2050 thermogravimetric analyzer. The sample was heated at a  $10^\circ\text{C}/\text{min}$  heating rate from  $40^\circ\text{C}$  to  $800^\circ\text{C}$ . Differential scanning calorimetry (DSC) was conducted under nitrogen on a TA Instruments 2100 differential scanning calorimeter. The sample was heated at  $10^\circ\text{C}/\text{min}$  from  $40^\circ\text{C}$  to  $300^\circ\text{C}$ .

Atomic force microscopy (AFM) (Advanced Scanning Probe Microscope, XE-100) operating in non-contact mode was used to image surface morphology. Two-dimensional X-ray diffraction was performed at room temperature. Cross-coupled parallel focusing mirrors were used to monochromate the X-ray radiation. The data were collected at still mode with 60 s per frame and processed with GADDS software. A stack of polymer films for two-dimensional X-ray diffraction studies was prepared by forming a polymer thin film on the wall of a round-bottomed flask *via* vacuum evaporation of a dilute polymer solution in chloroform.

Field-effect transistors based on PBDT-10 films were fabricated in a top-contact on a common gate of highly *n*-doped silicon with a 300 nm thick thermally grown  $\text{SiO}_2$  dielectric layer. The octadecyltrichlorosilane monolayer was treated in toluene solution for 2 h. Solutions of the organic

semiconductors were spin-coated at 3000 rpm from 0.2 wt %. Gold source and drain electrodes were evaporated on top of the semiconductor layers (100 nm). For all measurements, we used channel lengths (L) of 100  $\mu\text{m}$  and channel widths (W) of 1000  $\mu\text{m}$ . The electrical characteristics of the TFTs were measured in air using Keithley 4200. Field-effect mobilities were extracted in the saturation regime from the slope of the source-drain current.

**Materials.** 3-Bromothiophene was purchased from TCI. *n*-Butyllithium was purchased from Aldrich. Tetrakis(triphenylphosphine)palladium was purchased from Strem. All reagents purchased commercially were used without further purification. The tetrahydrofuran (THF) and diethyl ether were distilled from sodium benzophenone ketyl. Toluene was dried over calcium hydride.

**Synthesis of Thiophene-3-carbaldehyde.** To solution of 3-bromothiophene (50 g, 0.31 mol) in 500 mL of diethyl ether, a 2.5 M solution of *n*-BuLi in hexane (184 mL, 0.46 mol) was added at  $-78^\circ\text{C}$  under nitrogen. After 30 min of stirring at  $-78^\circ\text{C}$ , the yellow solution was added into a well stirred mixture of 33.6 g of *N,N*-dimethyl formaldehyde. The reaction mixture was warmed to room temperature and stirred for 12 h. After hydrolyzing with 500 mL of ice-water and 2 N HCl, the organic layer was extracted with ethyl ether and washed with aqueous sodium bicarbonate ( $\text{NaHCO}_3$ ) solution, and water until neutral. The organic phase was dried over anhydrous magnesium sulfate ( $\text{MgSO}_4$ ) and reduced solvent. The white liquid product was purified by vacuum distillation, with yield of 70% (21 g). bp  $42\text{--}44^\circ\text{C}$ .  $^1\text{H-NMR}$  (300 MHz,  $\text{CDCl}_3$ )  $\delta$  9.56 (s, 1H), 8.15 (s, 1H), 7.57 (d, 1H), 7.41 (d, 1H).

**Synthesis of 5-Bromothiophene-3-carbaldehyde.** Thiophene-3-carbaldehyde (6.5 g, 0.06 mol) was dissolved in 200 mL of dichloromethane (dry), and 14 g of aluminum chloride was added. The dark solution was stirred for 10 min and solution of bromine (10 g, 0.066 mol) in 10 mL of dichloromethane was added dropwise over 10 min period. The mixture was stirred for 12 h and poured onto crush-ice. The organic layer was separated and extracted with 2 N HCl, washed by water. The organic phase was dried over anhydrous  $\text{MgSO}_4$  and reduced solvent. The white liquid product was purified by vacuum distillation, with yield of 88% (10 g).  $^1\text{H-NMR}$  (300 MHz,  $\text{CDCl}_3$ )  $\delta$  9.50 (s, 1H), 7.45 (d, 1H), 7.29 (d, 1H).

**Synthesis of 1-(5-Bromothiophen-3-yl)-undecan-1-ol.** A Grignard reagent of 1-(magnesiumbromide) decane, prepared by the reaction of 1-bromodecane (17.3 g, 0.78 mol) with magnesium (5 g, 0.21 mol) in 50 mL of tetrahydrofuran (THF) was added drop wise into solution of 5-bromothiophene-3-carbaldehyde (9.1 g, 0.048 mol) in 150 mL of THF at  $0^\circ\text{C}$ . After stirring at room temperature for 10 min, the reaction mixture was treatment with water and 2 N HCl, stirred for 2 h. After evaporation of solvent, the mixture was extracted by dichloromethane. The organic phase was washed with water, dried over anhydrous  $\text{MgSO}_4$  and removed solvent. The pure product was obtained by a silica gel using a mixed solvent hexane and ethyl acetate (1:20, v/v) as

eluent, with yield of 63% (10 g).  $^1\text{H-NMR}$  (300 MHz,  $\text{CDCl}_3$ )  $\delta$  7.07 (s, 1H), 7.03 (s, 1H), 4.66 (t, 1H), 2.05 (s, 1H, OH), 1.27 (t, 18H,  $\text{CH}_2$ ), 0.92 (t, 3H,  $\text{CH}_3$ ).

**Synthesis of 2,6-Dibromo-4,8-didecyl-dithienobenzene.** To solution of 1-(5-bromothiophen-3-yl)-undecan-1-ol (1 g, 0.003 mol) in 200 mL of dichloromethane, a boron trifluoride-diethyl etherate (2 mL, 0.014 mol) in 5 mL of dichloromethane was added at  $-78^\circ\text{C}$  over 1 h period under nitrogen. The mixture was warmed to room temperature and stirred for 4 days. After hydrolyzing with 500 mL of ice-water and 2 N HCl, the organic layer was washed with  $\text{NaHCO}_3$  solution, and water. The organic phase was dried over anhydrous  $\text{MgSO}_4$  and removed solvent. The product was purified on silica gel using hexane as eluent. The pure product was obtained from recrystallization in isopropanol, with yield 10% (0.8 g).  $^1\text{H-NMR}$  (300 MHz,  $\text{CDCl}_3$ )  $\delta$  7.43 (s, 2H), 3.00 (t, 4H,  $\text{CH}_2$ ), 1.43 (t, 32H,  $\text{CH}_2$ ), 0.91 (t, 6H,  $\text{CH}_3$ ).

**Synthesis of 5,5'-Bis(tri-*n*-butylstannyl)-2,2'-bithiophene.** It was prepared according to literature<sup>28</sup> with yield of 88%.  $^1\text{H-NMR}$  (300 MHz,  $\text{CDCl}_3$ )  $\delta$  7.28 (d, 2H), 7.04 (d, 2H), 1.33 (m, 12H,  $\text{CH}_2$ ), 1.30 (m, 24H,  $\text{CH}_2$ ), 0.96 (m, 18H,  $\text{CH}_3$ ).

**Synthesis of Poly(4,8-didecylidithienobenzene-*alt*-dithiophene) (PBDT-10).** All handling of catalyst and polymerization were done in a nitrogen atmosphere. To a stirred mixture of 4,8-didecyl-2,6-dibromodithienobenzene (0.15 g, 0.24 mmol), 5,5'-bis(tri-*n*-butylstannyl)-2,2'-bithiophene (0.17 g, 0.23 mmol) in 45 mL of toluene (dry) was added. After bubbling by nitrogen gas for 30 min, catalyst (0.013 g, 5% mol) was added. The reaction mixture was refluxed for 12 h. A mixture of amount of trimethyl-naphthalene-2-yl-stannane and 2-bromo-naphthalene (an accesses 0.02 mol %) in 1 mL of toluene was added into the reaction mixture for end-capping for 6 h. The reaction mixture was terminated by pouring into 400 mL of methanol and 2 N-HCl. Precipitation was purified by soxhlet in methanol, acetone, hexane, chloroform and toluene as eluent. Copolymer was precipitated several times in methanol. The pure copolymer was dried over in vacuum oven to obtain 0.09 g to bright red powder. Yield: 58% (0.08 g).  $^1\text{H-NMR}$  (300 MHz,  $\text{CDCl}_3$ )  $\delta$  7.43 (s, 2H), 7.23 (s, 2H), 7.11 (s, 2H), 3.01 (t, 4H,  $\text{CH}_2$ ), 1.12-1.43 (t, 32H,  $\text{CH}_2$ ), 0.89 (t, 6H,  $\text{CH}_3$ ). FT-IR (KBr) ( $\text{cm}^{-1}$ ): 2926 (aromatic C-H), 2847 (aliphatic,  $\text{CH}_2$ ), 1643 (C=S in benzo-dithiophene), 1465 (C=S in dithiophene), 1222, 1156-788.

## Results and Discussion

The synthesis scheme of PBDT-10 was shown in Figure 1. The PBDT-10 was synthesized by Stille coupling. The copolymer was purified in order by soxhlet, extraction with methanol, acetone, hexane, and chloroform. The structure of polymer was confirmed by  $^1\text{H-NMR}$  and IR. The polymer has good solubility in chlorobenzene, and dichlorobenzene while it was soluble chloroform, toluene, tetrahydrofuran with heating at  $40^\circ\text{C}$ . The weight-average molecular weight ( $M_w$ ) of PBDT-10 was measured to be 8,400 with PDI of 1.4 by GPC in THF as eluent using the calibration curve of

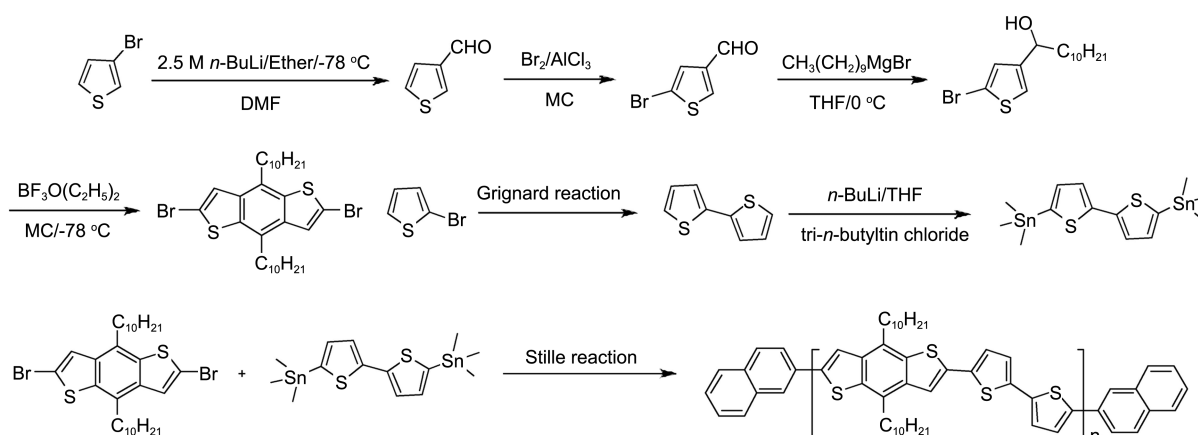


Figure 1. Synthetic scheme of poly(4,8-didecyl-dithienobenzene-*alt*-dithiophene) (PBDT-10).

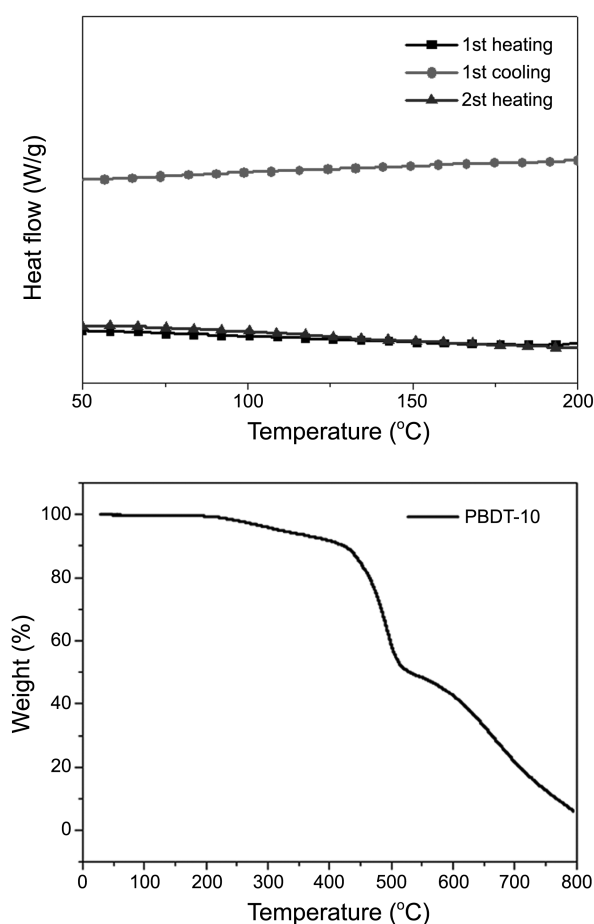


Figure 2. TGA and DSC curves of PBDT-10.

polystyrene standards.

The thermal properties of the polymer were determined by thermogravimetric analysis (TGA) under nitrogen. PBDT-10

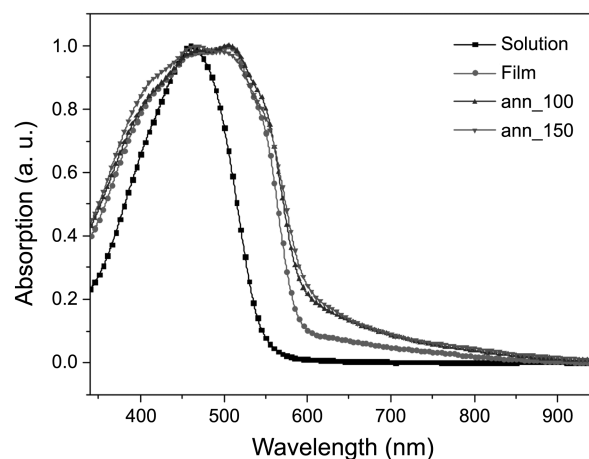


Figure 3. UV-vis absorption of PBDT-10 in chloroform, in the film state, and annealed film state.

has good thermal stability up to 324 °C (thermal decomposition temperature, Td). The glass transition temperature (Tg) was confirmed by differential scanning calorimetry (DSC). The Tg of the PBDT-10 was around 130 °C (Fig. 2).

Figure 3 shows normalized UV-vis absorption of a solution (CHCl<sub>3</sub>), film and annealed film. UV-vis absorption maximum appears at 462 nm for solution, and 471 and 506 nm for thin film. UV-vis absorption of PBDT-10 in film exhibited broad and red shift compared with that of solution, which means the strong inter chain interactions in the solid state.<sup>29</sup> The absorption spectrum was slightly broadened after annealing, which also means enhanced intermolecular interaction. The optical properties of the PBDT-10 were summarized in Table 1.

Electrochemical study was conducted by means of CV. The oxidation onset was occurred at +1.03 eV, which correspond to HOMO of 5.50 eV with Eox of ferrocene as

Table 1. Maximum UV absorption and electrochemical properties of PBDT-10

	Solution (max) (nm)	Film (max) (nm)	Film 100 ann (max) (nm)	Film 150 ann (max) (nm)	Edge (nm)	Bandgap (optical) (eV)	HOMO (electronic) (eV)	LUMO (optical) (eV)
PBDT-10	462	471,506	471,506	415,465,501	598	2.07	5.50	3.43

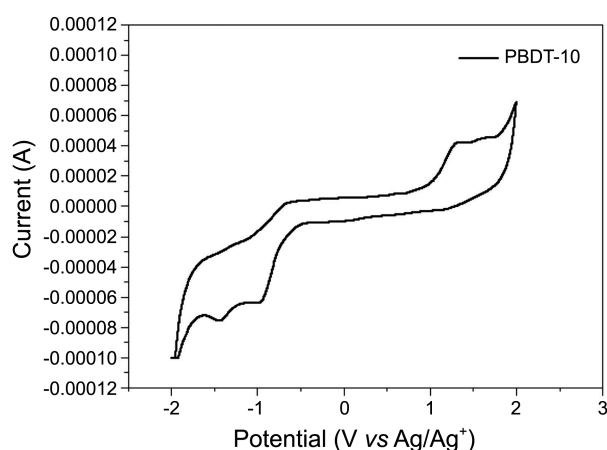


Figure 4. Cyclic voltammogram of PBDD-10.

standard. The optical band gap was estimated to be 2.07 eV from the absorption edge (598 nm), and calculated LUMO level was 3.43 eV (Fig. 4).

Non-contact mode AFM was utilized to observe the surface morphological structure of the film and the phase images are shown in Figure 5. The AFM of PBDD-10 exhibits the non-homogeneous thin film state. The film was not fully covered. This result may be attributed to the low molecular weight of polymer.

Also, to understand the arrangement of the PBDD-10, we carried out X-ray diffraction (XRD) analysis on thin film according to temperature. Strong (100) reflection peak was observed at respectively  $2\theta = 5.4^\circ$  (Fig. 6), indicating an ordered structure with d-spacing of 16.35 Å, which is ascribable to the interchain separation of the alkyl side chain. With annealing temperature increasing, from room temperature to 100 °C, and further to 150 °C, the film clearly shows a diffraction peak with relatively high intensity. The intensity of the peak continuously increases to a maximum value after annealing at 150 °C. The PBDD-10 film produces structurally more ordered arrangement of the polymer molecules, during the annealing process. The result of crystallinity is directly related to the mobility of PBDD-10.

OTFT devices were fabricated by using thin film of PBDD-10 with a top-contact device. The thin film transistors exhibit type p-channel TFT characteristics in the transfer and output curves. The mobility ( $\mu_{\text{FET}}$ ) and threshold voltage ( $V_{\text{TH}}$ ) of the OTFTs were obtained from saturation regimes

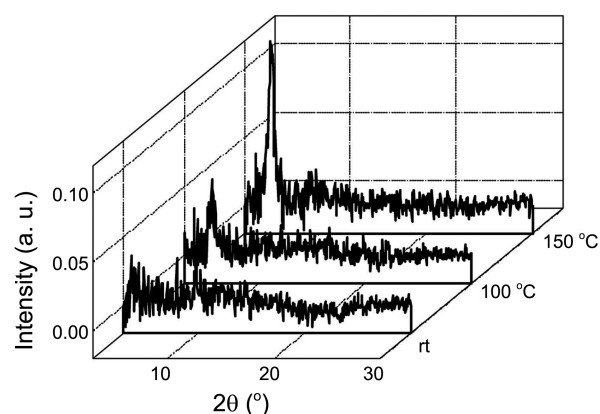


Figure 6. XRD images of PBDD-10 (a) at room temperature (b) at 100 °C, and (c) at 150 °C.

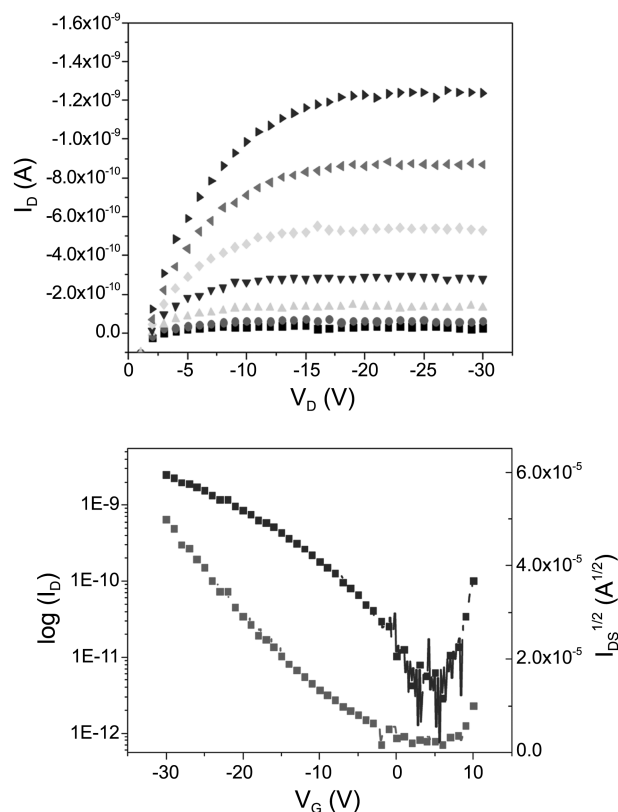


Figure 7. Output curve and drain current ( $I_D$ ) vs drain-source voltage ( $V_D$ ) characteristics of PBDD-10 at 150 °C annealing temperature.

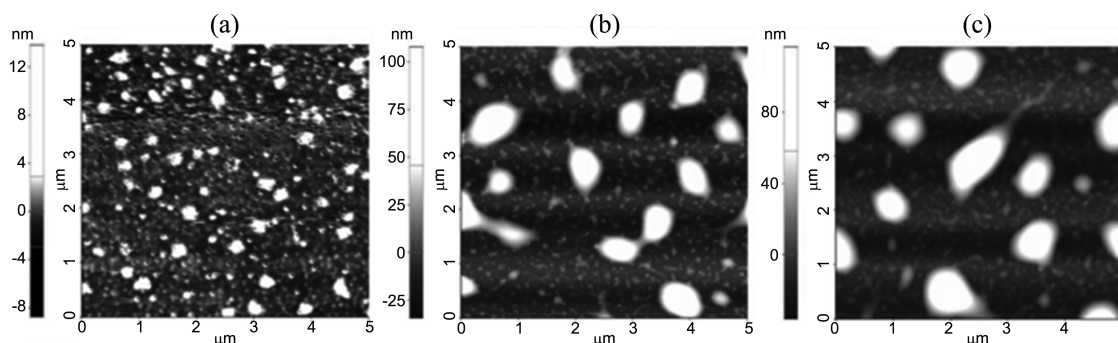


Figure 5. Atomic force microscopy images for film of PBDD-10 (a) at room temperature (b) at 100 °C, and (c) at 150 °C.

**Table 2.** Performance of TFTs based on PBDT-10

PBDT-10	$\mu_{\text{hole}}$ [ $\text{cm}^2/\text{Vs}$ ]	$I_{\text{on}}/I_{\text{off}}$	$V_{\text{th}}$ [V]	Sub [V/dec]
Fresh	-	-	-	-
100 ann	$6.1 \times 10^{-5}$	$4.54 \times 10^6$	-3.5	1.36
150 ann	$7.2 \times 10^{-5}$	$2.41 \times 10^3$	-4.8	0.74

using  $I_{\text{D}}^{\text{sat}} = (W/2L)\mu_{\text{FET}}C_i(V_{\text{G}} - V_{\text{TH}})^2$ , where  $L$  is the channel length,  $W$  is the channel width, and  $C_i$  is the capacitance per unit area of the gate dielectric layer ( $C_i = 10 \text{ nF/cm}^2$  for 300 nm thick  $\text{SiO}_2$ ). The output characteristics showed very good saturation behavior and clear saturation currents. The TFT performance of those devices was optimized by the variation of both substrate temperature and deposition speed. The hole mobility of PBDT-10 was  $6.1 \times 10^{-5} \text{ cm}^2 \text{ V}^{-1} \text{ s}^{-1}$  with subthreshold swing (ss) of 1.36 V/dec and  $I_{\text{on}}/I_{\text{off}}$  of  $4.64 \times 10^6$  from 100 °C annealing temperature while the mobility of PBDT-10 was not measured in the room temperature. The maximum hole mobility on solution-processed film was up to  $7.2 \times 10^{-5} \text{ cm}^2 \text{ V}^{-1} \text{ s}^{-1}$ , a threshold voltage of -4.8 V, subthreshold swing (ss) of 0.74 V, off current of  $1.03 \times 10^{-12}$  and  $I_{\text{on}}/I_{\text{off}}$  of  $2.41 \times 10^3$  from 150 °C annealing temperature (Fig. 7). The mobilities and  $I_{\text{on}}/I_{\text{off}}$  are summarized in Table 2. The high mobility at 150 °C annealing can be explained by increased intermolecular interaction due to increased molecular ordering.

### Conclusion

We were developed a p-type organic semiconducting polymer based on benzodithiophene (PBDT-10) by Stille coupling reaction. The PBDT-10 was shown the mobility enhancement according to the thermal annealing. It was confirmed that the crystallinity is increasing with annealing temperature through XRD images. The annealing process at the optimum temperature of 150 °C results in the highest hole mobility of  $7.2 \times 10^{-5} \text{ cm}^2 \text{ V}^{-1} \text{ s}^{-1}$  with a threshold voltage of -4.8 V and  $I_{\text{on}}/I_{\text{off}}$  of  $2.41 \times 10^3$ .

**Acknowledgments.** This work was funded by Korea Research Council of Fundamental Science and Technology (KRCF) and Korea Institute of Science and Technology (KIST) for “NAP National Agenda Project Program” and by the National Research Foundation of Korea Grant founded by the Korean Government 2012-047047.

### References

- Bae, J. H.; Park, J. H.; Keum, C. M.; Kim, W. H.; Kim, M. H.; Kim, S. O.; Kwon, S. K.; Lee, S. D. *Organic Electronics* **2010**, *11*, 784.
- Jackson, T. N.; Lin, Y. Y.; Gundlach, D. J.; Klauk, H. *IEEE J. Sel. Top. Quantum Electron.* **1998**, *4*, 100.
- Byun, C. W.; Son, S. W.; Lee, Y. W.; Kang, H. M.; Park, S. A.; Lim, W. C.; Li, T.; Joo, S. K. *Electron. Mater. Lett.* **2012**, *8*, 107.
- Qiao, Y.; Guo, Y.; Yu, C.; Zhang, F.; Xu, W.; Liu, Y.; Zhu, D. *J. Am. Chem. Soc.* **2012**, *134*, 4084.
- Park, H. T.; Shin, D. C.; Shin, S. C.; Kim, J. H.; Kwon, S. K.; Kim, Y. H. *Macromolecular Research* **2011**, *19*, 965.
- Chung, D. S.; Lee, S. J.; Park, J. W.; Choi, D. B.; Lee, D. H.; Park, J. W.; Shin, S. C.; Kim, Y. H.; Kwon, S. K.; Park, C. E. *Chem. Mater.* **2008**, *20*, 3451.
- Kim, S. O.; An, T. K.; Chen, J.; Kang, I.; Kang, S. H.; Chung, D. S.; Park, C. E.; Kim, Y. H.; Kwon, S. K. *Adv. Funct. Mater.* **2011**, *21*, 1616.
- Kwon, J. Y.; Lee, D. J.; Kim, K. B. *Electron. Mater. Lett.* **2011**, *7*, 1.
- Oh, D. H.; Zhao, Q. H.; Kim, S. O.; Park, H. T.; Kim, Y. H.; Park, Y. S.; Kim, J. J.; Kwon, S. K. *Macromolecular Research* **2011**, *19*, 629.
- Kwon, J. H.; Yeo, H. D.; Cha, H. J.; Lee, M. J.; Park, H. T.; Park, J. H.; Park, C. E.; Kim, Y. H. *Macromolecular Research* **2011**, *19*, 197.
- Chung, D. S.; Park, J. W.; Park, J. H.; Moon, D. H.; Kim, G. H.; Lee, H. S.; Lee, D. H.; Shim, H. K.; Kwon, S. K.; Park, C. E. *J. Mater. Chem.* **2010**, *20*, 524.
- Chung, S. J.; Kim, S. O.; Kwon, S. K.; Lee, C. H.; Hong, Y. T. *IEEE Electron Devices Letters* **2011**, *32*, 1134.
- Huang, H.; Youn, J.; Ortiz, R. P.; Zheng, Y.; Facchetti, A.; Marks, T. *Chem. Mater.* **2011**, *23*, 2185.
- Li, Z.; Zhang, Y.; Tsang, S. W.; Du, X.; Zhou, J.; Tao, Y.; Ding, J. *J. Phys. Chem. C* **2011**, *115*, 18002.
- Pan, H.; Li, Y.; Wu, Y.; Liu, P.; Ong, B. S.; Zhu, S.; Xu, G. *J. Am. Chem. Soc.* **2007**, *129*, 4112.
- Pan, H.; Li, Y.; Wu, Y.; Liu, P.; Ong, B. S.; Zhu, S.; Xu, G. *Chem. Mater.* **2006**, *18*, 3237.
- Park, J. W.; Lee, D. H.; Chung, D. S.; Kang, D. M.; Kim, Y. H.; Park, C. E.; Kwon, S. K. *Macromolecules* **2010**, *43*, 2118.
- Chung, D. S.; Park, J. W.; Kim, S. O.; Heo, K. Y.; Park, C. E.; Ree, M. H.; Kim, Y. H.; Kwon, S. K. *Chem. Mater.* **2009**, *21*, 5500.
- Rieger, R.; Beckmann, D.; Pisula, W.; Steffen, W.; Kastler, M.; Müllen, K. *Adv. Mater.* **2010**, *22*, 83.
- Ong, B. S.; Wu, Y. L.; Li, Y. N.; Liu, P.; Pan, H. L. *Chem. Eur. J.* **2008**, *14*, 4766.
- McCulloch, I.; Heeney, M.; Bailey, C.; Genevicius, K.; Macdonald, I.; Shkunov, M.; Sparrowe, D.; Tierney, S.; Wagner, R.; Zhang, W. M.; Chabinyc, M. L.; Kline, R. J.; McGehee, M. D.; Toney, M. F. *Nat. Mater.* **2006**, *5*, 328.
- Li, J.; Qin, F.; Li, C. M.; Bao, Q.; Park, M. B. C.; Zhang, W.; Qin, J.; Ong, B. S. *Chem. Mater.* **2008**, *20*, 2057.
- Price, S. C.; Stuart, A. C.; You, W. *Macromolecules* **2010**, *43*, 797.
- Sista, P.; Biewer, M. C.; Stefan, M. C. *Macromol. Rapid Commun.* **2012**, *33*, 9.
- Price, S. C.; Stuart, A. C.; Yang, L.; Zhou, H.; You, W. *J. Am. Chem. Soc.* **2011**, *133*, 4627.
- Shi, Q.; Fan, H.; Liu, Y.; Hu, W.; Li, Y.; Zhan, X. *Macromolecules* **2011**, *44*, 9173.
- Kim, S. O.; Lee, M. W.; Jang, S. H.; Park, S. M.; Park, J. W.; Park, M. H.; Kang, S. H.; Kim, Y. H.; Song, C. K.; Kwon, S. K. *Thin Solid Films* **2011**, *519*, 7998.
- McCullough, R. D.; Lowe, R. D.; Jayaraman, M.; Anderson, D. L. *J. Org. Chem.* **1993**, *58*, 904.
- Jang, S. H.; Tai, T. B.; Park, J. H.; Jeong, H. J.; Chun, E. J.; Kim, Y. H.; Lee, S. G. *Macromolecular Research* **2010**, *18*, 189.